Int. J. of Applied Mechanics and Engineering, 2006, vol.11, No.3, pp.623-637

STEADY AND UNSTEADY BOUNDARY LAYERS DUE TO A STRETCHING VERTICAL SHEET IN A POROUS MEDIUM USING DARCY-BRINKMAN EQUATION MODEL

A. ISHAK and R. NAZAR*
School of Mathematical Sciences, National University of Malaysia
43600 UKM Bangi, Selangor, MALAYSIA
e-mail: rmn72my@yahoo.com

I. POP
Faculty of Mathematics, University of Cluj
R-3400 Cluj, CP 253, ROMANIA

The present paper deals with the analysis of a steady and unsteady boundary layer flow and heat transfer past a vertical stretching sheet in a viscous fluid-saturated porous medium by using the Darcy-Brinkman equation model. It is assumed that unsteadiness is caused by the impulsive stretching of the sheet and by a sudden increase in the surface temperature. The problem is reduced to parabolic partial differential equations, which are solved numerically using the Keller-box method. The small time (initial unsteady flow) as well as the large time (final steady-state flow) solutions are also included in the analysis. It is shown that there is a smooth transition from the small time solution to large time solution, respectively.

Key words: steady and unsteady boundary layers, stretching vertical sheet, porous medium, Darcy-Brinkman equation model.

1. Introduction

The production of sheeting material, which includes both metal and polymer sheets arises in a number of industrial manufacturing processes. The fluid dynamics due to a stretching surface is important in many extrusion processes. For many practical applications, the stretching surfaces undergo cooling or heating that cause surface velocity and temperature variations. Since the pioneering study by Crane (1970) who presented an exact analytical solution for the steady two-dimensional stretching of a surface in a quiescent fluid, many authors have considered various aspects of this problem and obtained similarity solutions. The recent papers by Magyari and Keller (1999; 2000), Liao and Pop (2004) and Nazar *et al.* (2004) contain a good amount of references on this problem. On the other hand, the boundary layer flow due to a stretching surface in the vertical direction in a steady, viscous and incompressible fluid when the buoyancy forces are taken into account has only been considered in the papers by Daskalakis (1993), Ali and Al-Yousef (1998), Chen (1998, 2000), Lin and Chen (1998) and Chamkha (1999). However, to the best of our knowledge, only Kumari *et al.* (1996) and Ishak *et al.* (2005) have studied the unsteady free and mixed convection flow, respectively, over a stretching vertical surface in an ambient fluid. Both constant surface temperature and constant surface heat flux conditions have been considered.

Recently, Liu and Wang (2005) have studied the steady flow and heat transfer of a viscous fluid-saturated porous medium past a permeable and non-isothermal sheet with internal heat generation or absorption using the Darcy-Brinkman equations model. The unsteady case has been studied by Sharidan *et al.* (2005). It is well known that Darcy's law is an empirical formula relating the pressure gradient, the bulk viscous resistance and the gravitational force for a convective flow in a porous medium. Deviations from Darcy's law occur when the Reynolds number based on the pore diameter it within the range of 1 to 10. For

* To whom correspondence should be addressed

a flow through a porous medium with high permeability, Brinkman (1947) as well as Chen *et al.* (1992), argue that the momentum equation must reduce to the viscous flow limit and advocate that classical frictional terms be added in Darcy's law. Vafai and Tien (1981), and Kaviany (1987) used the Darcy-Brinkman model to study the effects of boundary and inertia forces on forced convection over a fixed impermeable heated plate embedded in a porous medium. They defined a momentum boundary layer as the layer adjacent to the surface where the viscous effect on the surface and the bulk viscous force are equally important. The existence of the momentum boundary layer near the heated surface was shown to retard the streamwise velocity close to the wall, resulting in a decrease of the surface heat flux.

The aim of this paper is to study the steady and unsteady flow and heat transfer past a stretching sheet in a vertical direction placed in a fluid-saturated porous medium using the Darcy-Brinkman equation model. In view of industrial applications, it is interesting to examine the flow and thermal characteristics of viscous fluids over a stretching sheet in a porous medium. In the physical process of drawing a sheet from a slit of a container, it is tacitly assumed that only the fluid adhered to the sheet is moving but the porous matrix remains fixed to cope the usual assumption of flow motion in a porous medium. For a fluid through an isotropic and homogeneous porous medium, we apply the general equations modeled by Vafai and Tien (1981), and Hsu and Cheng (1990), with neglecting the quadratic terms from the momentum equations. It is assumed that both the stretching velocity and surface temperature vary linearly with the distance along its surface. It is also assumed that the unsteadiness is caused by the impulsive stretching of the sheet and by sudden increase in the surface temperature. The governing partial differential equations are transformed into a non-dimensional form using similarity and semi-similarity variables, and the transformed equations are then solved numerically using the Keller-box method, which is an implicit finite-difference scheme.

2. Problem formulation and basic equations

We assume that two equal and opposite forces are impulsively applied along the *x*-axis of a vertical stretching sheet, keeping the origin fixed, the sheet being placed in a fluid-saturated porous medium of ambient temperature T_∞. It is also assumed that the temperature $T_w(x)$ of the sheet is suddenly increased or decreased to the value T_∞. The stationary coordinate system has its origin located at the center of the sheet with the positive *x*-axis extending along the sheet, while the *y*-axis is measured normal to the surface of the sheet, respectively (see Fig.1).

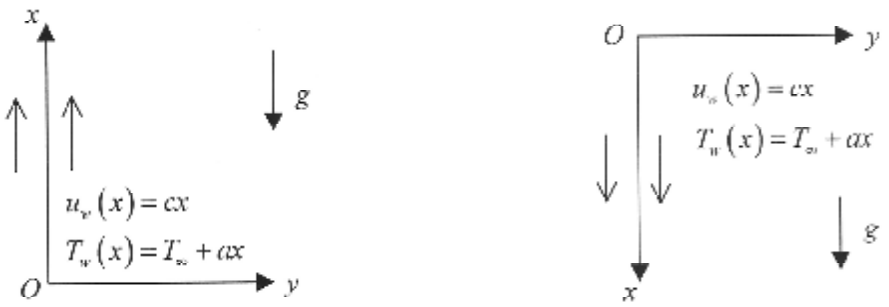

(a) Assisting flow (b) Opposing flow

Fig.1. Physical model and coordinate system.

The continuous stretching surface is assumed to have the velocity of the form $u_w(x) = c\,x$ and temperature $T_w(x) = T_\infty + a\,x$ where a and c are constants with $c > 0$. Under these assumptions along with the Darcy-Brinkman equation model and boundary layer approximations, the basic boundary layer equations are (Nakayama, 1995)

$$\frac{\partial u}{\partial x}+\frac{\partial \nu}{\partial y}=0, \tag{2.1}$$

$$\rho_f\left(\frac{\partial u}{\partial t}+u\frac{\partial u}{\partial x}+\nu\frac{\partial u}{\partial y}\right)=\tilde{\mu}\frac{\partial^2 u}{\partial y^2}-\frac{\mu}{K_1}\phi u+\rho_f g\beta(T-T_\infty), \tag{2.2}$$

$$(\rho_f c_p)\phi\left(\frac{\partial T}{\partial t}+u\frac{\partial T}{\partial x}+\nu\frac{\partial T}{\partial y}\right)=k_m\frac{\partial^2 T}{\partial y^2}, \tag{2.3}$$

subject to the initial and boundary conditions

$$\begin{aligned} &t<0: \quad u=0, && T=T_\infty, && \text{for any} \quad x,y,\\ &t\geq 0: \quad u=u_w(x)=cx, && \nu=0, && T=T_w(x)=T_\infty+ax \quad \text{at} \quad y=0,\\ &\qquad\quad u\to 0, && T\to T_\infty && \text{as} \quad y\to\infty \end{aligned} \tag{2.4}$$

where t is time, u and v are the velocity components along the x- and y- axes, respectively, T is the temperature, ρ_f, $\tilde{\mu}$, μ, ϕ and K_1 are the fluid density, effective dynamic viscosity, dynamic viscosity, porosity and permeability, respectively. As we have already mentioned, the resistance quadratic inertial term or inertia loss term in Eq.(2.2) have been neglected.

(i) *Steady-state case*

In this case, $\partial/\partial t=0$ and we look for a similarity solution of the steady-state Eqs (2.1)-(2.3) of the form

$$\psi=(c\mu/\rho_f)^{1/2}x\,f(\eta), \quad \theta(\eta)=(T-T_\infty)/(T_w-T_\infty), \quad \eta=(c\rho_f/\mu)^{1/2}y \tag{2.5}$$

where ψ is the free stream defined in the usual way as $u=\partial\psi/\partial y$ and $\nu=-\partial\psi/\partial x$. Substituting (2.5) into Eqs (2.2) and (2.3) we get the following ordinary differential equations

$$\Lambda f'''+ff''-f'^2-Kf'+\lambda\theta=0, \tag{2.6}$$

$$\frac{1}{\Pr}\theta''+f\theta'-f'\theta=0, \tag{2.7}$$

subject to the boundary conditions

$$f(0)=0, \quad f'(0)=1, \quad \theta(0)=1, \quad f'(\infty)=0, \quad \theta(\infty)=0 \tag{2.8}$$

where primes denote differentiation with respect to η. The constant parameter Λ is the viscous ratio parameter, K is the porous medium parameter and λ is the buoyancy force parameter which are defined as

$$\Lambda=\frac{\tilde{\mu}}{\mu}, \quad K=\frac{\mu\phi}{c\rho_f K_1}, \quad \lambda=\frac{\mathrm{Gr}_x}{\mathrm{Re}_x^2}, \tag{2.9}$$

respectively, where $\mathrm{Gr}_x = g\beta(T_w - T_\infty)x^3/\nu^2$ is the local Grashof number and $\mathrm{Re}_x = u_w x/\nu$ is the local Reynolds number, respectively. It is worth mentioning that both assisting $(\lambda > 0)$ and opposing $(\lambda < 0)$ flow cases are considered.

(ii) *Unsteady-state flow case*

Following Seshadri *et al.* (2002) or Nazar *et al.* (2004), we introduce now the following non-dimensional variables

$$\psi = (c\mu/\rho_f)^{1/2} x\xi^{1/2} f(\xi,\eta), \quad \theta(\xi,\eta) = (T - T_\infty)/(T_w - T_\infty),$$
$$\eta = (c\rho_f/\mu)^{1/2}\xi^{-1/2} y, \quad \xi = 1 - e^{-\tau}, \quad \tau = ct, \tag{2.10}$$

for $0 \le \xi \le 1$. With the use of Eq.(2.10), Eqs (2.2) and (2.3) become

$$\Lambda f''' + (1-\xi)\frac{\eta}{2} f'' + \xi\left(ff'' - f'^2 - Kf' + \lambda\theta\right) = \xi(1-\xi)\frac{\partial f'}{\partial \xi}, \tag{2.11}$$

$$\frac{1}{\mathrm{Pr}}\theta'' + (1-\xi)\frac{\eta}{2}\theta' + \xi f\,\theta' - \xi f'\theta = \xi(1-\xi)\frac{\partial \theta}{\partial \xi}, \tag{2.12}$$

subject to

$$f(\xi,0) = 0, \quad f'(\xi,0) = 1, \quad \theta(\xi,0) = 1,$$
$$f'(\xi,\eta) \to 0, \quad \theta(\xi,\eta) \to 0, \quad \text{as} \quad \eta \to \infty, \tag{2.13}$$

for $0 \le \xi \le 1$, where primes denote partial differentiation with respect to η.

For the unsteady-early flow case, where $\xi \approx 0$, Eqs (2.11) and (2.12) are approximately reduced to the following form

$$\Lambda f''' + \frac{\eta}{2} f'' = 0, \quad \frac{1}{\mathrm{Pr}}\theta'' + \frac{\eta}{2}\theta' = 0, \tag{2.14}$$

subject to the boundary conditions (2.8). The solution to this problem is given by

$$f'(\eta) = \mathrm{erfc}\left(\frac{\eta}{2\sqrt{\Lambda}}\right), \quad f(\eta) = \eta\,\mathrm{erfc}\left(\frac{\eta}{2\sqrt{\Lambda}}\right) + 2\sqrt{\frac{\Lambda}{\pi}}\left[1 - \exp\left(-\frac{\eta^2}{4\Lambda}\right)\right],$$
$$\theta(\eta) = \mathrm{erfc}\left(\sqrt{\mathrm{Pr}}\,\eta/2\right) \tag{2.15}$$

where erfc (.) is the complimentary error function.

On the other hand, for the final steady-state flow case, where $\xi = 1$, Eqs (2.11) and (2.12) reduce to Eqs (2.6) and (2.7), respectively.

The physical quantity of interest in this problem includes the skin friction coefficient, C_f, and the local Nusselt number, Nu_x, which are defined as

$$C_f = \frac{\tau_w}{\rho_f u_w^2}, \qquad \mathrm{Nu}_x = \frac{x q_w}{k_m (T_w - T_\infty)}, \tag{2.16}$$

respectively, where

$$\tau_w = \tilde{\mu}\left(\frac{\partial u}{\partial y}\right)_{y=0}, \qquad q_w = -k_m\left(\frac{\partial T}{\partial y}\right)_{y=0}. \tag{2.17}$$

Using variables (2.10), it is easily shown that C_f and Nu_x can be expressed as

$$C_f \mathrm{Re}_x^{1/2} = \Lambda \xi^{-1/2} f''(\xi, 0), \qquad \mathrm{Nu}_x / \mathrm{Re}_x^{1/2} = -\xi^{-1/2}\theta'(\xi, 0), \tag{2.18}$$

for $0 \le \xi \le 1$.

3. Results and discussion

The two sets of Eqs (2.6)-(2.7) and (2.11)-(2.12) subject to the boundary conditions (2.8) and (2.13), respectively, were solved numerically using the Keller-box finite-difference method described by Cebeci and Bradshaw (1988). Results were obtained for $\Lambda = 1$ and some values of the parameters, i.e., the Prandtl number, Pr, buoyancy force parameter, λ, and porous material parameter, *K*, with values of ξ in the range $0 \le \xi \le 1$. Both assisting $(\lambda > 0)$ and opposing $(\lambda < 0)$ flow cases are considered. Numerical results for skin friction coefficient $C_f \mathrm{Re}_x^{1/2}$, local Nusselt number $\mathrm{Nu}_x / \mathrm{Re}_x^{1/2}$, velocity profiles $f'(\eta)$, as well as the temperature profiles $\theta(\eta)$ are obtained.

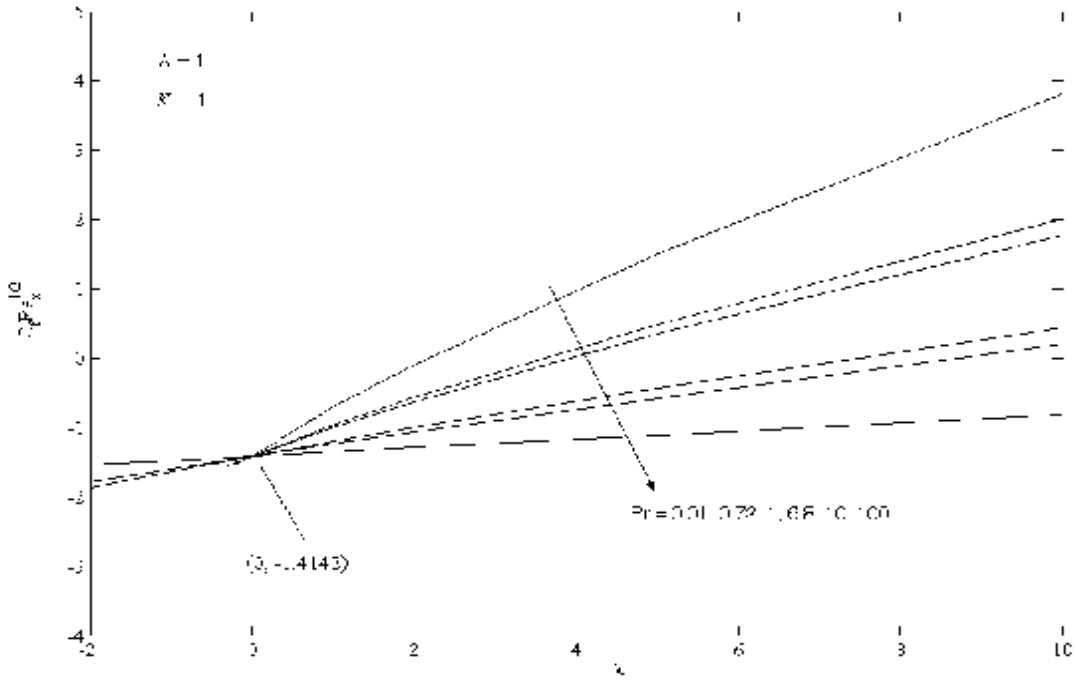

Fig.2. Skin friction coefficient $C_f \mathrm{Re}_x^{1/2}$ vs. λ for various values of Pr when $\Lambda = K = 1$, for the steady-state case.

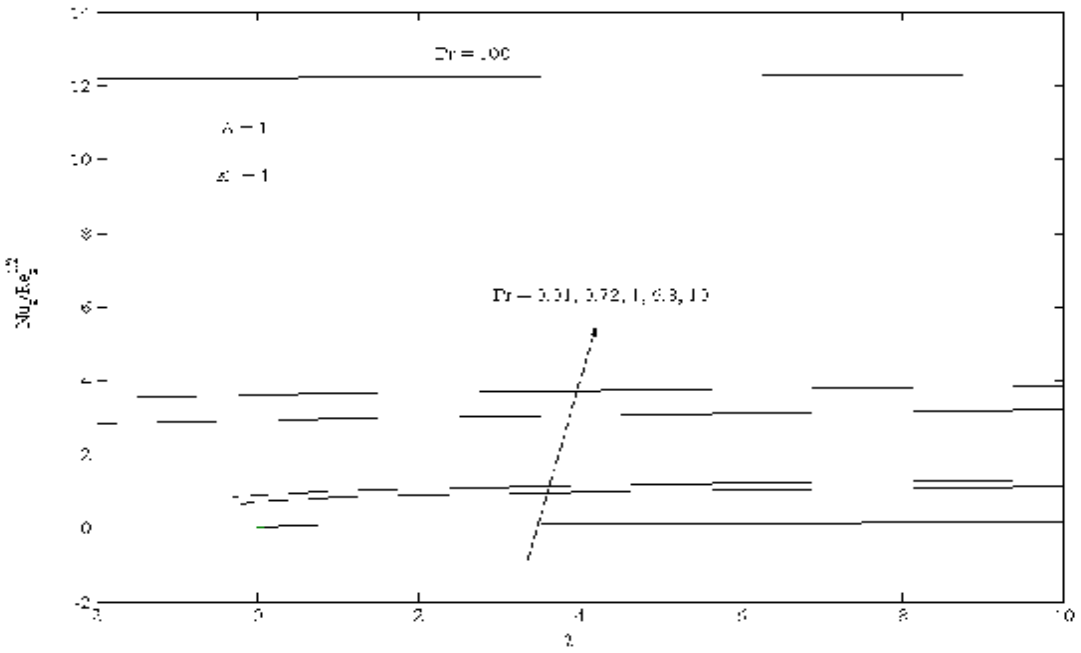

Fig.3. Local Nusselt number $\mathrm{Nu}_x/\mathrm{Re}_x^{1/2}$ vs. λ for various values of Pr when $\Lambda = K = 1$, for the steady-state case.

The results for the skin friction coefficient $C_f \mathrm{Re}_x^{1/2}$ and local Nusselt number $\mathrm{Nu}_x/\mathrm{Re}_x^{1/2}$ for the steady-state case as a function of λ for various Pr are presented in Figs 2 and 3, respectively. As can be seen from Fig.2, all curves intersect at a point where $\lambda = 0$; that is when the buoyancy force is zero. This is because Eqs (2.6) and (2.7) are uncoupled when $\lambda = 0$, in other words, the solutions to the flow field are not affected by the thermal field in which the buoyancy force is lacking. Also, the value of $C_f \mathrm{Re}_x^{1/2}$ remains constant, that is *-1.4142*, for all Pr, which agreed with the result obtained by Sharidan *et al.* (2005), who showed that $C_f \mathrm{Re}_x^{1/2} = -\sqrt{\Lambda(1+K)}$. It is observed from Fig.2 that a positive buoyancy force $(\lambda > 0)$ produces an increase in the skin friction coefficient, while a negative buoyancy force $(\lambda < 0)$ gives rise to a decrease in the skin friction coefficient. This is because the fluid velocity increases when buoyancy force increases and hence increases the skin friction. The opposite trend occurs when buoyancy force decreases. Also, effects of λ on the skin friction coefficient are found to be more significant for fluids having smaller Pr since the viscosity is less than that of the fluids with larger Pr. Thus, fluids with a smaller Pr are more sensitive to the buoyancy force than fluids with a larger Pr. From Tab.1 and Fig.6, it can be seen that the skin friction coefficient decreases when the porous material parameter K increases. This is clear from the fact that the porosity ϕ increases when K increases, which causes the increasing of the void space in the medium. Thus, the wall shear stress decreases which then causes the decreasing of the skin friction coefficient.

The variations of the local Nusselt number as a function of the buoyancy force parameter λ for the steady-state case is shown in Fig.3. It is observed from this figure that for a particular value of Pr, the local Nusselt number is slightly increased as the buoyancy force parameter is increased. Also, Fig.3 shows that for a particular value of Pr, the local Nusselt number is slightly increased as the buoyancy parameter λ is increased, since in this problem the fluid is always converted from colder to warmer wall portions (in Fig.1 both arrows point in the direction of increasing values of the wall coordinate x). However, in the opposing

flow case, the volume flux of the colder fluid transported is smaller than in the assisting flow case (since in the former case the buoyancy forces work against the sheer forces induced by the stretching wall). Accordingly, for all values of Pr, the amount of heat that can be transferred per second from the unit surface of the wall to the moving fluid is necessarily smaller in the opposing case than in the assisting case. In addition, the effects of Pr can be examined, that is, for a fixed value of λ the local Nusselt number increases with Pr, because the higher Prandtl number a fluid has the lower thermal conductivity (or the higher viscosity) is, which results in a thinner thermal boundary layer and hence, a higher heat transfer rate at the surface. From Tab.2, it is observed that for a fixed Prandtl number, the increasing of a porous material parameter K causes the local Nusselt number to decrease. This is clear from the fact that the increasing of porous material parameter causes the porosity ϕ to increase, which enhances the void space in the medium, and in turn reduces the surface heat transfer rate.

Table 1. Skin friction coefficient, $C_f \mathrm{Re}_x^{1/2}$, for various values of K and Pr at $\xi = 1$ when $\Lambda = \lambda = 1$.

Pr \ K	0.1	0.5	1	2	3	4	5
0.01	-0.1645	-0.4258	-0.7028	-1.1429	-1.4894	-1.7801	-2.0341
0.72	-0.5631	-0.7530	-0.9625	-1.3176	-1.6163	-1.8775	-2.1118
1	-0.6110	-0.7960	-1.0000	-1.3467	-1.6397	-1.8968	-2.1281
6.8	-0.8423	-1.0183	-1.2089	-1.5301	-1.8017	-2.0414	-2.2584
10	-0.8743	-1.0503	-1.2404	-1.5603	-1.8307	-2.0691	-2.2848
100	-0.9887	-1.1646	-1.3541	-1.6721	-1.9403	-2.1766	-2.3902

Table 2. Local Nusselt number, $\mathrm{Nu}_x / \mathrm{Re}_x^{1/2}$, for various values of K and Pr at $\xi = 1$ when $\Lambda = \lambda = 1$.

Pr \ KK	0.1	0.5	1	2	3	4	5
0.01	0.0980	0.0900	0.0813	0.0684	0.0596	0.0534	0.0488
0.72	0.9006	0.8659	0.8278	0.7643	0.7140	0.6724	0.6374
1	1.0773	1.0405	1.0000	0.9323	0.8772	0.8311	0.7917
6.8	3.0467	3.0040	2.9573	2.8775	2.8099	2.7498	2.6953
10	3.7373	3.6944	3.6478	3.5686	3.5010	3.4405	3.3859
100	12.3165	12.2732	12.2265	12.1479	12.0814	12.0226	11.9694

Figures 4-7 show the variations of the skin friction coefficient $C_f \mathrm{Re}_x^{1/2}$ and the local Nusselt number $\mathrm{Nu}_x / \mathrm{Re}_x^{1/2}$ with ξ (unsteady-state case) for some values of λ and K by solving Eqs (2.11) and (2.12) numerically. The steady-state solution $(\xi = 1)$ obtained by solving Eqs (2.6) and (2.7) are also included in these figures. The effect of λ and K on the skin friction coefficient and the local Nusselt number are consistent with the steady-state case mentioned in the previous paragraph. It is noticed that there is a very good agreement between the results when the full unsteady state equations and the steady state

equations are solved. It is also noticed that the transition from unsteady to steady flows takes place smoothly.

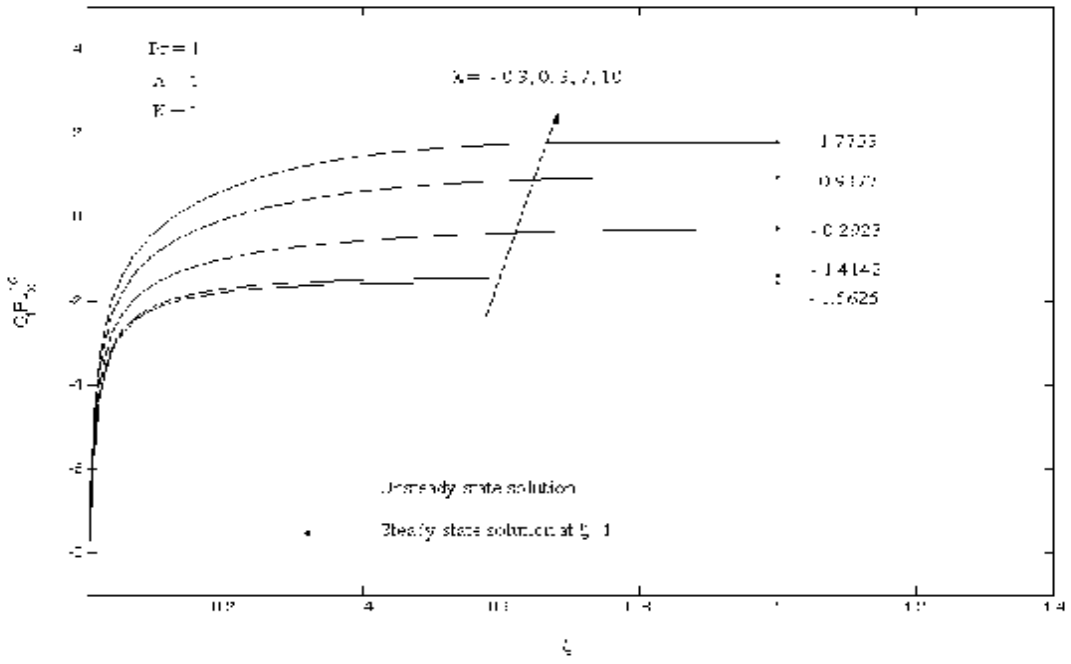

Fig.4. Skin friction coefficient, $C_f \mathrm{Re}_x^{1/2}$, at selected values of λ for $\mathrm{Pr} = 1$, $\Lambda = 1$, $K = 1$.

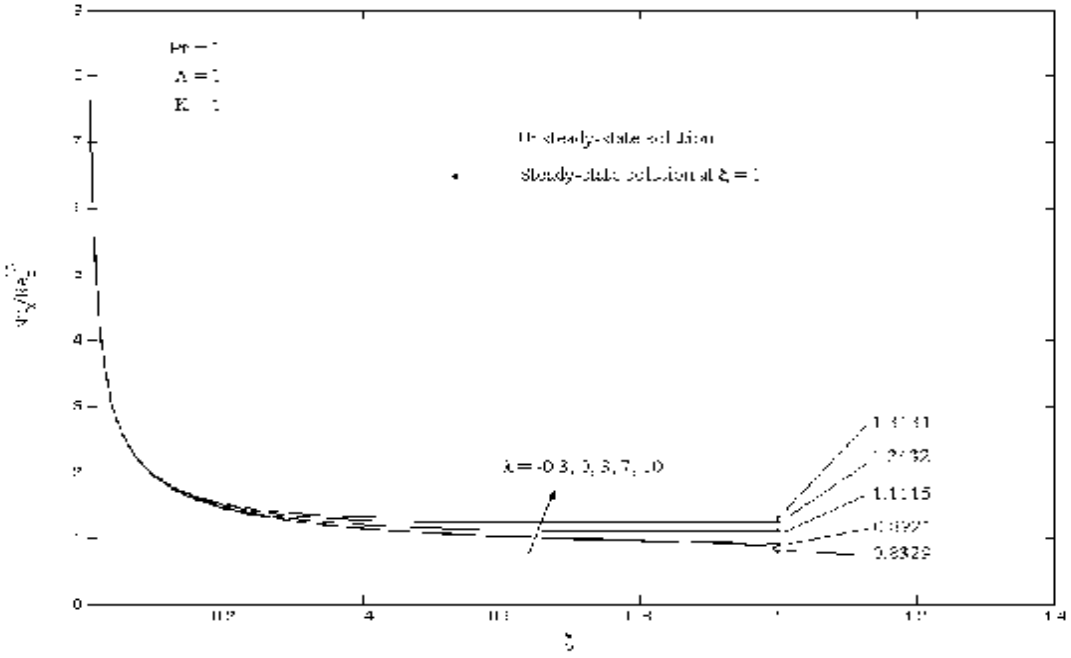

Fig.5. Local Nusselt number, $\mathrm{Nu}_x / \mathrm{Re}_x^{1/2}$, at selected values of λ for $\mathrm{Pr} = 1$, $\Lambda = 1$, $K = 1$.

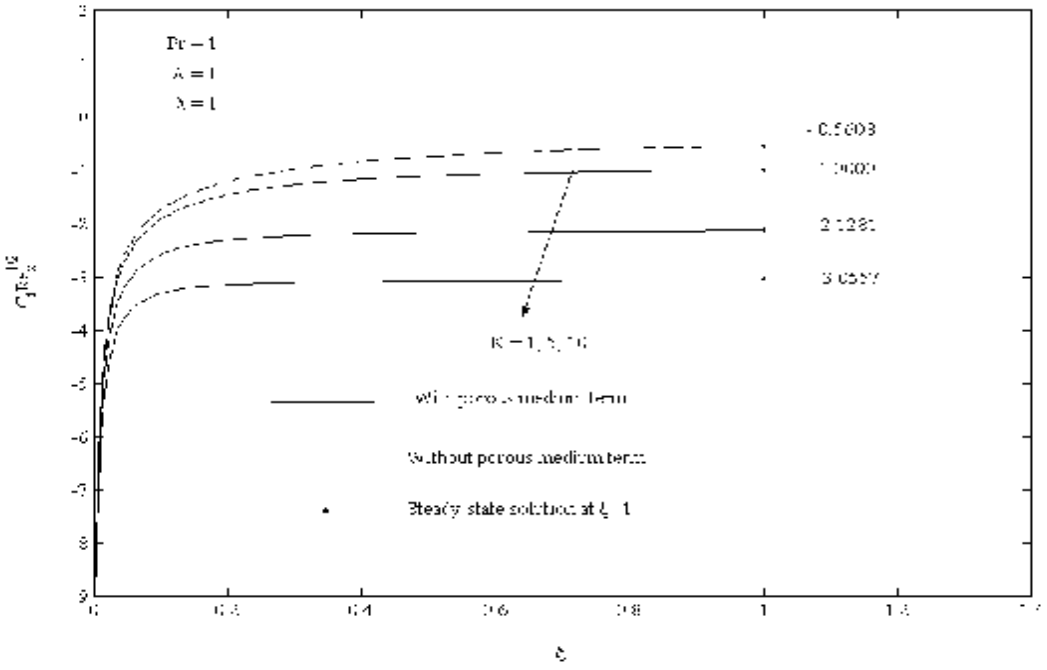

Fig.6. Skin friction coefficient, $C_f \mathrm{Re}_x^{1/2}$, at selected values of K for $\mathrm{Pr} = 1$, $\Lambda = 1$, $\lambda = 1$.

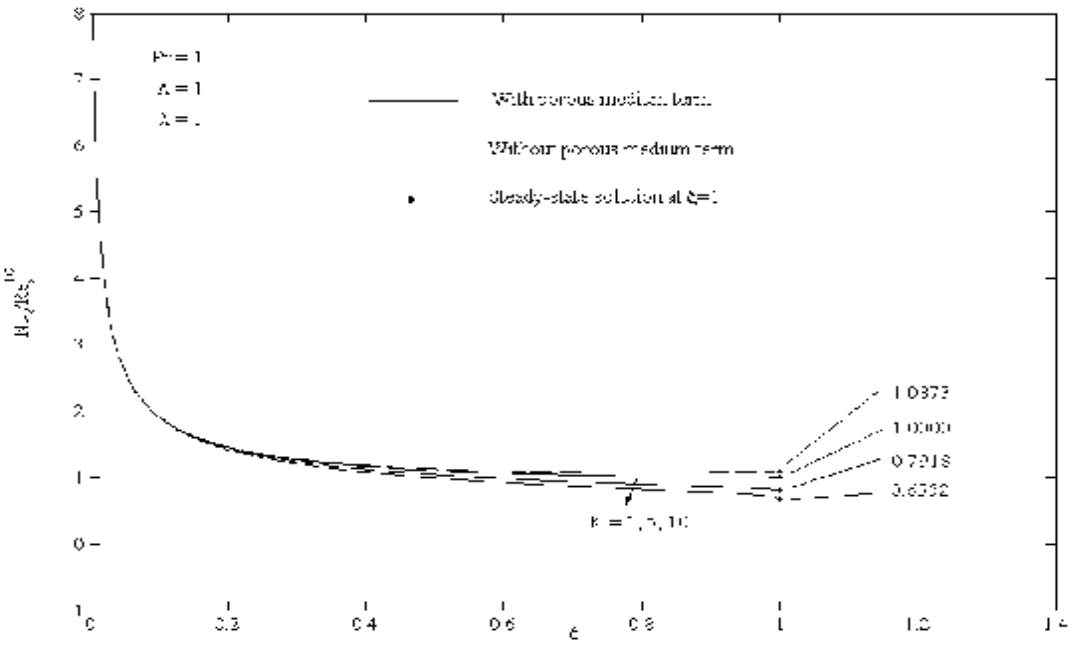

Fig.7. Local Nusselt number, $\mathrm{Nu}_x / \mathrm{Re}_x^{1/2}$, at selected values of K for $\mathrm{Pr} = 1$, $\Lambda = 1$, $\lambda = 1$.

The evolution of the dimensionless velocity profiles $f'(\eta)$ and dimensionless temperature profiles $\theta(\eta)$ are shown for various values of λ, K and Pr in Figs 8-13, respectively. For the dimensionless velocity profiles, the effects of K or Pr is such that the velocity boundary layer thickness decreases slightly with an

increase in K or Pr. The effect of Pr on the dimensionless temperature profiles is such that the thermal boundary layer thickness decreases sharply with an increase in Pr, and hence induces an increase in the surface temperature gradient. The opposite trend occurs for the porous material parameter, K; that is the thermal boundary layer thickness increases with an increase in K. It is also noticed that for a fixed Pr and K, an increase in λ will result in decreasing temperature.

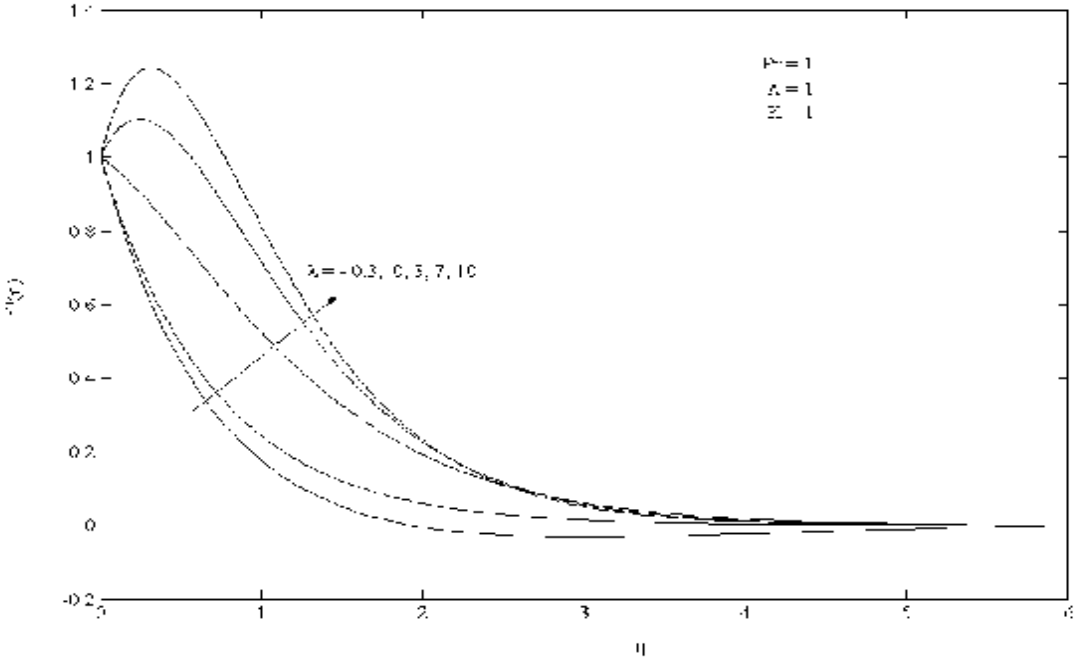

Fig.8. Velocity profiles, $f'(\eta)$, at selected values of λ for $\Pr = 1$, $\Lambda = 1$, $K = 1$.

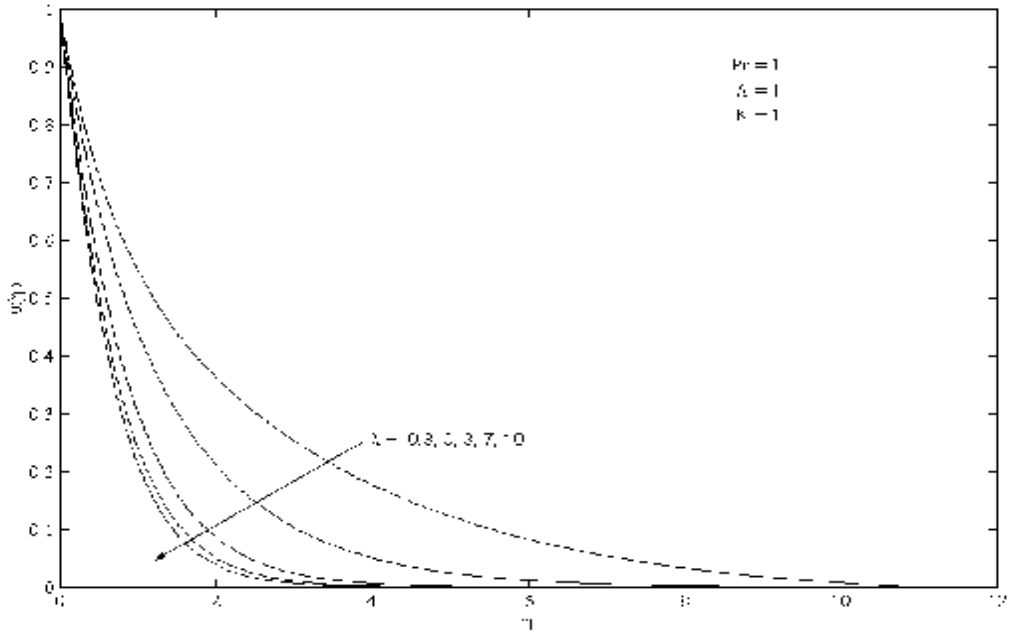

Fig.9. Temperature profiles, $\theta(\eta)$, at selected values of λ for $\Pr = 1$, $\Lambda = 1$, $K = 1$.

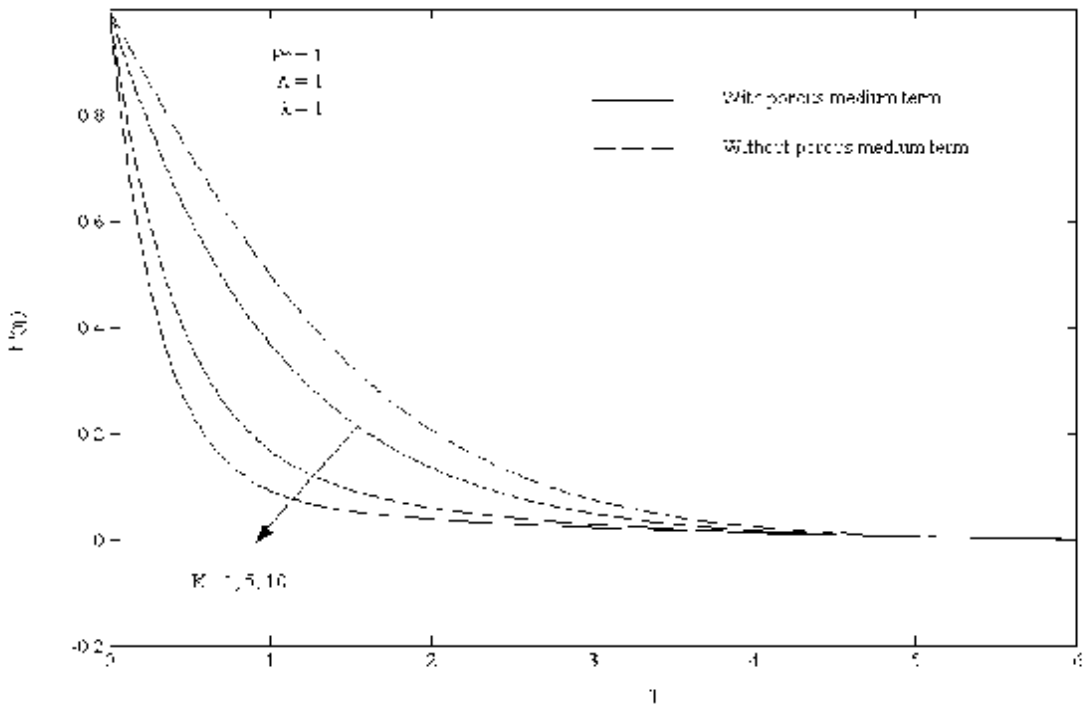

Fig.10. Velocity profiles, $f'(\eta)$, at selected values of K for $\Pr = 1$, $\Lambda = 1$, $\lambda = 1$.

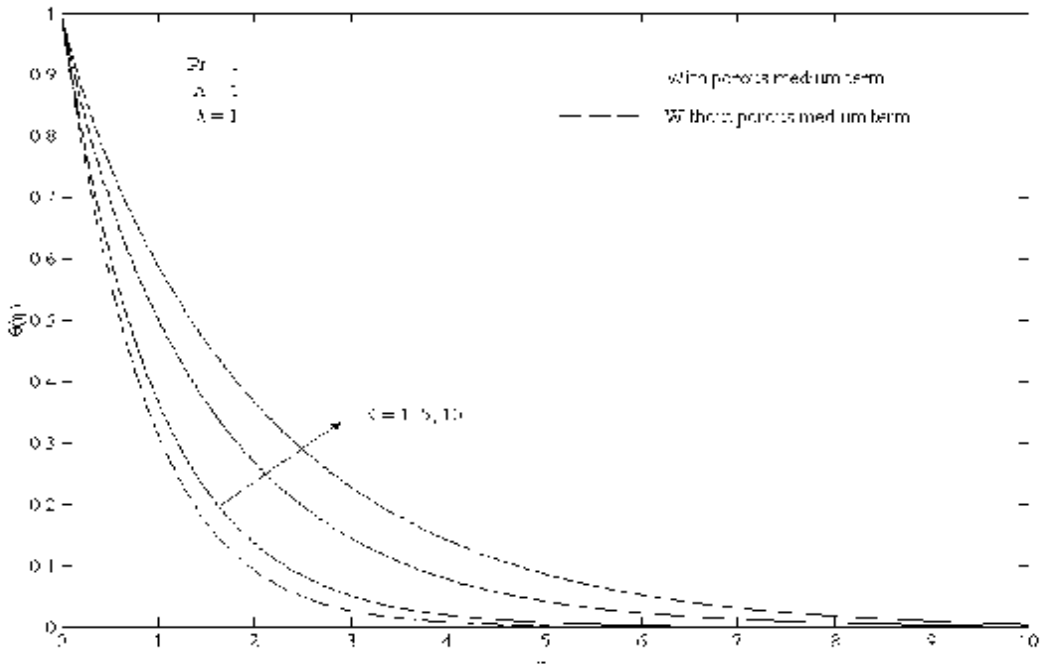

Fig.11. Temperature profiles, $\theta(\eta)$, at selected values of K for $\Pr = 1$, $\Lambda = 1$, $\lambda = 1$.

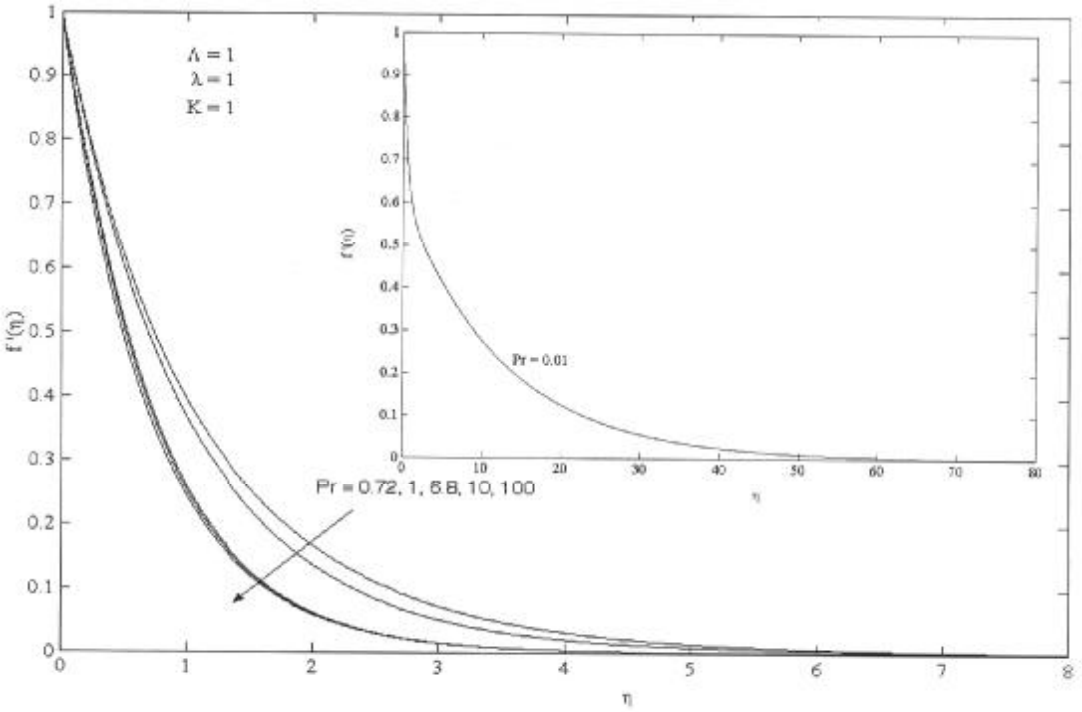

Fig.12. Velocity profiles, $f'(\eta)$, at selected values of Pr for $\mathrm{Pr} = 1$, $\Lambda = 1$, $\lambda = 1$.

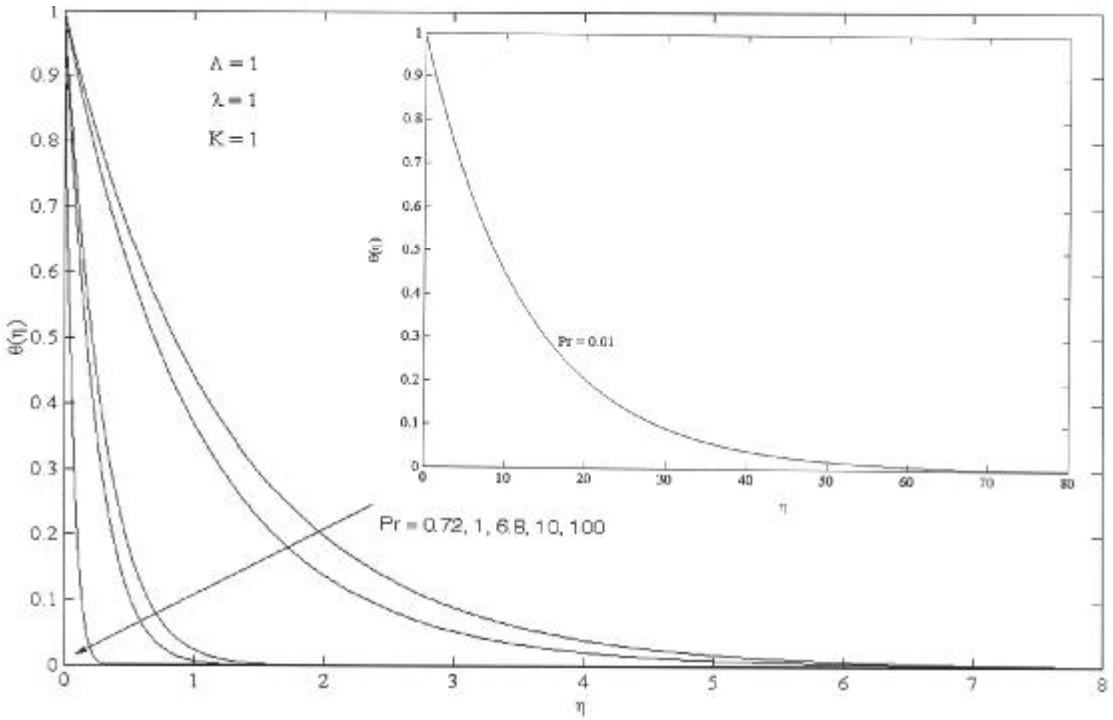

Fig.13. Temperature profiles, $\theta(\eta)$, at selected values of Pr for $\mathrm{Pr} = 1$, $\Lambda = 1$, $\lambda = 1$.

The resulting profiles of dimensionless velocity $f'(\eta)$ for various values of λ, K and Pr are illustrated in Figs 8, 10 and 12, respectively. From Fig.8, it can be noted that for large values of λ, the velocity increases at the beginning until it achieves a certain value, then decreases until the value becomes zero at the outside of the boundary layer. This is because a large value of λ produces a large buoyancy force, which produces large kinetic energy. Then the energy is used to overcome resistance along the flow, which becomes zero far away from the surface. Sauch a trend does not occur for a small value of λ, as can be seen from Figs 10 and 12, which is for $\lambda = 1$. The velocity decreases monotonically for all values of K and Pr when the distance from the surface increases. Figure 12 presents the effect of Pr on the velocity distribution. As shown, the velocity decreases as Pr increases since a higher Pr fluid has higher viscosity. Also, for a fixed value of λ and K, the boundary layer thickness decreases with an increase in Pr.

Figures 9, 11 and 13 present the temperature distribution for various values of λ, K and Pr, respectively. It is evident from these figures that the temperature of the fluid decreases monotonically as the distance from the surface increases, for all values of λ, K and Pr until it achieves a constant value, namely zero. This implies that the temperature gradually decreases with η. As shown in Figs 9, 11 and 13, an increase in λ and Pr results in a decrease in the thermal boundary layer thickness, respectively, whereas the opposite trend occurs for K, i.e., increasing value of K implies the increasing of the thermal boundary layer thickness. It is evident from Fig.9 that an increase in λ results in a decrease in the thermal boundary layer thickness, associated with an increase in the wall temperature gradient, and hence produces an increase in the surface heat transfer rate. It can be seen from Fig.13 that the temperature decreases as Pr increases. Also, for a fixed value of λ and K, the thermal boundary layer thickness increases with a decrease in Pr.

4. Conclusions

The present study provides both analytical and numerical solutions for the unsteady boundary layer flow and heat transfer of a viscous fluid-saturated porous medium past an impermeable and isothermal stretching sheet with internal heat generation or absorption using the Darcy-Brinkman equation model. The results show that the transition from the initial unsteady flow to the final steady-state flow takes place smoothly. The obtained results also show that the reduced skin friction increases, but the reduced heat transfer continuously decreases with time ξ. It was found, as expected, that the higher Prandtl number a fluid has, the thinner the thermal boundary is, which increases the gradient of temperature. Consequently, the surface heat transfer is increased as Pr increases. On the other hand, the skin friction decreases as Pr increases.

Acknowledgment

The authors gratefully acknowledged the financial support received in the form of a research grant (IRPA project code: 09-02-02-10038-EAR) from the Ministry of Science, Technology and Innovation (MOSTI), Malaysia.

Nomenclature

a, c – constants
C_f – local skin friction coefficient
c_p – specific heat at constant pressure
f – reduced stream function
g – acceleration due to gravity
Gr_x – local Grashof number
k_m – thermal conductivity

K – porous medium parameter
K_1 – permeability of the porous medium
Nu_x – local Nusselt number
Pr – Prandtl number
q_w – heat transfer from the stretching surface
Re_x – local Reynolds number
t – time
T – fluid temperature
$T_w(x)$ – temperature of the stretching surface
T_∞ – ambient temperature
u, v – velocity components along x and y directions, respectively
$u_w(x)$ – velocity of the stretching surface
x, y – Cartesian coordinates along the surface and normal to it, respectively
β – thermal expansion coefficient
ϕ – porosity
η – pseudo-similarity variable
λ – buoyancy force parameter
Λ – viscous ratio parameter
θ – dimensionless temperature
ν – kinematic viscosity
μ – dynamic viscosity
$\tilde{\mu}$ – effective dynamic viscosity
ρ_f – fluid density
τ – dimensionless time
τ_w – skin friction from the surface of the sheet
ξ – dimensionless transformed variable
ψ – stream function

Superscript

$'$ – differentiation with respect to η

Subscripts

w – condition at the wall
∞ – ambient condition

References

Ali M.E. and Al-Yousef F. (1998): *Laminar mixed convection from a continuously moving vertical surface with suction or injection.* – Heat Mass Transfer, vol.33, pp.301-306.

Brinkman H.C. (1947): *A calculation of the viscous force exerted by a flowing fluid on a dense swarm of particles*. – Appl. Sci. Res., vol.1, pp.27-34.

Cebeci T. and Bradshaw P. (1988): *Physical and Computational Aspects of Convective Heat Transfer*. – New York: Springer.

Chamkha A.J. (1999): *Hydromagnetic three-dimensional free convection on a vertical stretching surface with heat generation or absorption.* – Int. J. Heat Fluid Flow, vol.20, pp.84-92.

Chen C.-H. (1998): *Laminar mixed convection adjacent to vertical, continuously stretching sheets.* – Heat Mass Transfer, vol.33, pp.471-476.

Chen C.-H. (2000): *Mixed convection cooling of heated continuously stretching surface.* – Heat Mass Transfer, vol.36, pp.79-86.

Chen C.-K., Chen C.-H., Minkowycz, W.J. and Gill U.S. (1992): *Non-Darcian effects on mixed convection about a vertical cylinder embedded in a saturated porous medium.* – Int. J. Heat Mass Transfer, vol.35, pp.3041-3046.

Crane L.J. (1970): *Flow past a stretching plane*. – J. Appl. Math. Phys. (ZAMP), vol.21, pp.645-647.

Daskalakis J.E. (1993): *Free convection effects in the boundary layer along a vertically stretching flat surface.* – Canadian J. Phys., vol.70, pp.1253-1260.

Hsu C.T. and Cheng, P. (1990): *Thermal dispersion in a porous medium*. – Int. J. Heat Mass Transfer, vol.33, pp.1587-1597.

Ishak A., Nazar R. and Pop I. (2005): *Unsteady mixed convection boundary layer flow due to a stretching vertical surface* (submitted for publication).

Kaviany M. (1987): *Boundary-layer treatment of forced convection heat transfer from a semi-infinite flat plate embedded in porous media*. – J Heat Transfer, vol.109, pp.345-349.

Kumari M., Slaouti A., Takhar H.S., Nakamura S. and Nath G.. (1996): *Unsteady free convection flow over a continuously moving vertical surface.* – Acta Mechanica, vol.116, pp.75-82.

Liao S.-J. and Pop I. (2004): *Explicit analytic solution for similarity boundary layer equations*. – Int. J. Heat Mass Transfer, vol.47, pp.75-85.

Lin C.-R. and Chen C.-K. (1998): *Exact solution of heat transfer from a stretching surface with variable heat flux.* – Heat Mass Transfer, vol.33, pp.477-480.

Liu I.-C. and Wang H.-H. (2005): *Exact solutions for flow and heat transfer of a fluid-saturated porous medium over a permeable non-isothermal stretching sheet, without using boundary layer theory* (submitted for publication).

Magyari E. and Keller B. (1999): *Heat and mass transfer in the boundary layers on an exponentially stretching continuous surface*. – J. Phys. D: Appl. Phys., vol.32, pp.577-585.

Magyari E. and Keller B. (2000): *Exact solutions for self-similar boundary-layer flows induced by permeable stretching surfaces*. – Eur. J. Mech. B-Fluids, vol.19, pp.109-122.

Nakayama A. (1995): *PC-Aided Numerical Heat Transfer and Convective Flow*. – Tokyo: CRC Press.

Nazar R., Amin N. and Pop I. (2004): *Unsteady boundary layer flow due to a stretching surface in a rotating fluid.* – M.echanics Res. Comm., vol.31, pp.121-128.

Seshadri R., Sreeshylan N. and Nath G. (2002): *Unsteady mixed convection flow in the stagnation region of a heated vertical plate due to impulsively motion.* – Int. J. Heat Mass Transfer, vol.45, pp.1345-1352.

Sharidan S., Amin N. and Pop I. (2005): *Unsteady boundary layer due to a stretching sheet in a porous medium using Brinkman equation model* (submitted for publication).

Vafai K. and Tien C.L. (1999): *Boundary and inertia effects on flow and heat transfer in porous media.* – Int. J. Heat Mass Transfer, vol.24, pp.195-203.

Received: May 5, 2005

Revised: August 5, 2005